International Journal of Renewable Energy and Environmental Sustainability
Volume.7, Number 3;July-September, 2022;
ISSN: 2837-3391| Impact Factor:6.47
https://zapjournals.com/Journals/index.php/ijrees
Published By: Zendo Academic Publishing

LOW-TEMPERATURE PLASMA REACTOR FOR AMMONIA GAS TREATMENT: EXPERIMENTAL FINDINGS

Dr. Li Wei[1]

Article Info

Keywords: Waste Categorization, Foul Odors, Environmental Quality, Health Risks, Civic Engagement

Abstract

In contemporary society, a prevailing contradiction emerges from the escalating aspirations for an enhanced quality of life, set against a backdrop of uneven and insufficient development. The pursuit of an improved living environment and heightened environmental standards constitutes a paramount objective. As the imperative of waste categorization gains traction, individuals are gradually cultivating the commendable practice of conscientious waste sorting. Yet, the persistent issue of noxious odors in proximity to waste sorting and recycling facilities proves to be a formidable challenge. These malodorous emissions, which exert a potent olfactory assault, induce discomfort, hinder respiration, and instigate restlessness. Consequently, individuals often resort to covering their noses and hastily vacating the premises, impeding the efficacy of waste categorization efforts and substantially diminishing civic engagement. Concurrently, the adverse health repercussions of foul odors extend to residents inhabiting the vicinity of waste sorting and recycling centers. These odors not only elicit repugnance but also harbor substantial health hazards, impinging on respiratory, digestive, nervous, and endocrine systems, thereby potentially instigating chronic ailments that imperil human well-being [1].

Introduction

The main contradiction in current society is the increasing demand of the people for a better life, in contrast to the imbalanced and inadequate development. A good environmental quality and living environment are also goals we need to gradually pursue. With the issue of garbage classification gradually gaining popularity, people are gradually developing the good habit of taking pride in sorting their waste. However, due to the often accompanying foul odors at garbage sorting and recycling stations, which strongly stimulate people's olfactory organs and cause discomfort, it makes people feel difficulty in breathing and restless. They often cover their noses and hurriedly leave, making it difficult to effectively address garbage classification and significantly reducing residents' participation. At the same time, the foul odors have a significant impact on the health of residents living

[1] School of Engineering, Huazhong University of Science and Engineer, Wuhan, China

near garbage sorting and recycling stations. Foul odors not only have a nauseating smell, but also pose significant health risks, affecting people's respiratory system, digestive system, nervous system, and endocrine system, potentially leading to chronic diseases that harm human health. [1]

1. Experience Details

1.1 Equipment

The experimental setup used in this study is a Line-cartridge reactor, as shown in Figure 1. The reactor is housed in a specially designed stainless steel casing with a length of 120mm. To measure the removal efficiency at different reaction gaps, four reactors with inner diameters of 48mm, 56mm, 66mm, and 98mm were prepared. The two ends of the reactors were sealed with specially designed stainless steel flanges and plastic casings, and airtight sealing was achieved using black electrical tape. The reaction core consisted of 0.1mm titanium wire and four homemade reaction cores. During the reaction process, a corona zone of 120mm in length formed between the corona wire and the reactor tube after applying high-voltage direct current to the electrodes. The homemade reaction cores also formed corona fields due to self-sustained discharge at the tips of the metal foils.[2]

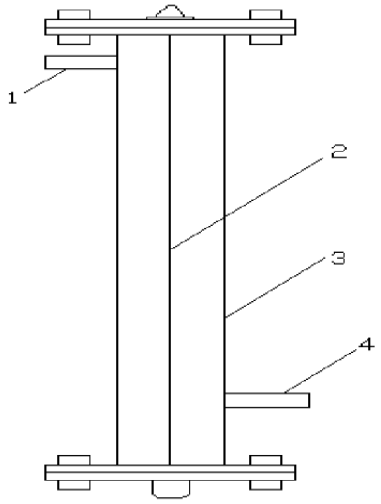

1. Air inlet 2. Corona wire 3. Stainless steel pipe 4. Air outlet

Figure 1: Line-cartridge reactor

The sizes of each reactor are shown in Table 1

Table 1: Sizes of each reactor

number	r/mm	l/mm	v/L
1	48	120	0.22
2	56	120	0.30
3	66	120	0.41
4	98	120	0.91

1.2 High voltage discharge device

To obtain stable high-voltage direct current, a high-voltage power supply was constructed according to the analog circuit shown in Figure 2.

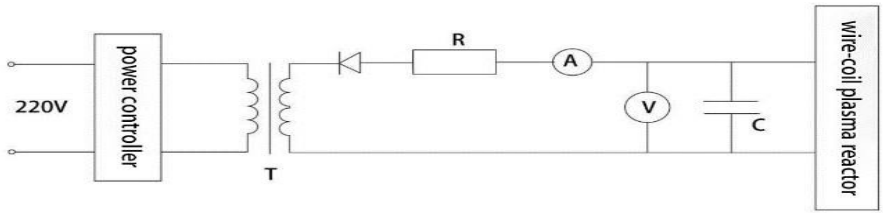

Figure 2: High-Voltage Circuit Diagram

First, the 220V AC power enters the power control box and passes through a transformer. The transformer converts the input AC voltage to high-voltage AC output, with a maximum output voltage of 50kV and output current of 200mA. At the output of the transformer, there is a silicon stack consisting of numerous diodes. The parameters of the high-voltage silicon stack are 0.1A and 200kV. These diodes convert the high-voltage AC to unstable unidirectional DC.

Next, to ensure a stable high voltage applied to the reactor, a homemade capacitor bank is connected in parallel across the reactor. The homemade capacitor bank is composed of eight 100kV, 10000PF capacitors connected in parallel.

Finally, a water resistor (R) is connected in series before the DC microammeter to ensure the safety of the microammeter. After each voltage boost, a large amount of charge accumulates in the capacitor bank.[3] At the end of the experiment, a grounding rod is connected to the circuit to discharge the charge in the capacitor bank to the ground. The grounding rod is connected in series with a 10Ω resistor to ensure the safety of the experiment. The assembled circuit is shown in Figure 3.

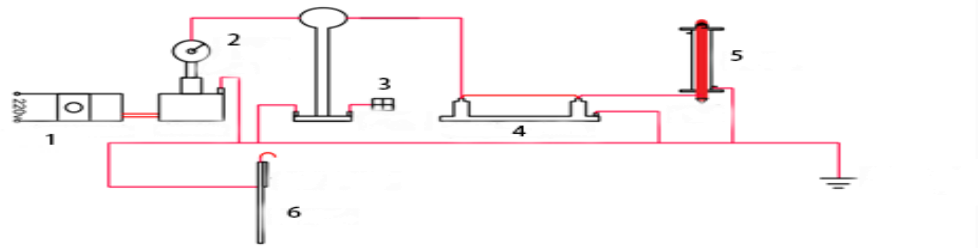

1. Voltage controller 2. Ammeter 3. Voltmeter 4. Parallel capacitor 5. Wire-coil plasma reactor 6. Grounding rod

Figure 3: Assembly circuit diagram

1.3 Experimental process

Firstly, in order to obtain the breakdown voltage and breakdown voltage of different reactor configurations with various discharge gaps and reactor cores, a volt-ampere characteristic analysis of the reactor needs to be conducted. This analysis will help determine the optimal reactor configuration. It serves as a preparatory step for subsequent experiments.

Secondly, computer analysis software will be used to analyze the electric field strength generated by self-sustained discharge in different reactor cores. [4] This analysis aims to explore the internal principles of the reactor and provide theoretical support for further experiments.

Finally, a gas flow experiment will be conducted to analyze the various factors that influence the process.

In this experiment, an ammonia gas is introduced into the reaction system using a fan equipped with a frequency modulator. The frequency of the modulator can be adjusted to control the output airflow of the fan, thereby altering the residence time of NH_3 gas in the reactor. A steel cylinder containing 5000 ppm of standard gas is used as the nitrogen source, and the flow of ammonia gas is adjusted by regulating the rotor flow meter connected to the cylinder. These two components are combined to achieve the desired ammonia gas concentration.

Subsequently, the thoroughly mixed NH_3 gas enters the linear-cylinder reactor, where rapid reactions occur under the influence of the low-temperature plasma generated in the high-voltage electric field. Gas samples are taken at the inlet of the reactor to measure the NH_3 concentration in the incoming gas. At the reactor outlet, samples are collected to measure the remaining NH_3 concentration and the concentration of the reaction products.[5]

A pump is used to evacuate gas at the inlet and outlet of the reactor, and a U-shaped tube absorber containing 50 ml of 0.01 mol/L sulfuric acid solution is employed to collect the gas. The residual exhaust gas from the reaction contains residual NH_3 and the main product NOX, which are collected in a gas collection tank.

The 0.01 mol/L sulfuric acid solution reacts with NH3 as follows to achieve the purpose of gas collection:

$$H\ H\ _2S\ S\ S\ S\ _4+2N\ N\ H\ H\ _3=(N\ N\ H\ H\ _4)_2S\ S\ S\ S\ _4 \quad (1)$$

1.4 Simulated exhaust gas preparation

1.4.1 Relationship between frequency and output air volume

This experiment uses the GZLING high-pressure blower, which has a linear relationship between the output airflow and input frequency. [6] The experimental results are shown in Table 2.

Table 2: Frequency-air volume relationship

f(Hz)	3	4	5	6	7
Q(L/min)	5.34	12.06	18.80	25.65	31.62

The relationship between the output airflow (Y) and the input frequency (X) of the blower is given by:

$$Y= 6.6152x - 14.382 \quad (2)$$

Here, Y represents the blower airflow in L/min, and X represents the blower frequency in Hz. This relationship is shown in Figure 4.

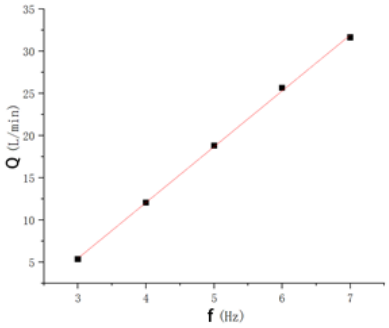

Figure 4: Output airflow-frequency relationship diagram

1.4.2 Simulate the intake air concentration of exhaust gases

The concentration of the simulated malodorous gas used in the experiment is a mixture of air and standard NH_3 gas. The standard NH_3 gas with a concentration of 5000 ppm is contained in a high-pressure cylinder, and its pressure is used to push the gas into the gas pipeline, where it mixes with the ambient air and enters the mixing chamber. The NH_3 gas concentration range prepared for this experiment is 30-90 ppm.[7] The calculation formula for the inlet concentration, based on mass conservation, is as follows:

$$C\ C\ 0=C\ C\ \underline{1}Q\ Q\ Q\ Q\ \underline{1}1++C\ C\ Q\ Q\ \underline{2}2Q\ Q\ \underline{2} \quad (3)$$

Where;

C_0—Air intake concentration;ppm

C_1—NH_3 concentration in air= 0ppm;

Q_1—Fan flow;L/min

C_2—Gas cylinder exhaust gas concentration;ppm

Q_2—Gas cylinder flow;L/min

1.4.3 Simulate the residence time of exhaust gases

In order to better understand the effect of residence time on the removal efficiency of odorous gas in the reactor, the following formula is used to calculate the residence time in this experiment.[8]

$$t\,t = \frac{V\,V}{Q\,Q\,1+Q\,Q\,2}\times 60 \qquad (4)$$

Where:

t—residence time;s

V—Reactor volume;L

Q_1—fan flow; L/min

Q_2—NH_3 standard gas flow;L/min

During the gas preparation process, since Q2 << Q1, for the sake of calculation simplicity, Q1 can be approximated as Q1 + Q2 in Equation (2-5) to obtain the calculation formula for residence time.

$$t\,t = \frac{V\,V}{Q\,Q\,1}\times 60 \qquad (5)$$

1.4.4 Gas distribution concentration table

This study aims to experiment with three influencing factors: discharge voltage controlled by the power supply console, discharge gap varied by switching different reactors, residence time controlled by adjusting the fan flow rate, and inlet concentration controlled by adjusting the air-to-gas ratio. The experimental inlet concentrations were set at 30ppm, 45ppm, 60ppm, 75ppm, and 90ppm. The residence time was selected as 1s, 2s, 3s, and 4s. The discharge gaps were set at 24mm, 28mm, 33mm, and 49mm. [9] Combining Equations (2-4) and (2-5), the gas distribution table was calculated as shown in Table 3.

Table 3: Gas distribution meter (unit: L/min)

Discharge gap(mm)	V(L)	NH_3(ppm)		residence time/s			
				1	2	3	4
24	0.217147	Fan flow (L/min)		13.029	6.514	4.343	3.257
		Standard gas flow(L/min)	30	0.078	0.039	0.026	0.02
			45	0.117	0.059	0.039	0.029
			60	0.156	0.078	0.052	0.039
			75	0.195	0.098	0.065	0.049
			90	0.235	0.117	0.078	0.059
28	0.295561	Fan flow (L/min)		17.734	8.867	5.911	4.433
		Standard gas flow(L/min)	30	0.106	0.053	0.035	0.027
			45	0.16	0.08	0.053	0.04
			60	0.213	0.106	0.071	0.053
			75	0.266	0.133	0.089	0.067
			90	0.319	0.16	0.106	0.08
33	0.410543	Fan flow (L/min)		24.633	12.316	8.211	6.158
		Standard gas flow(L/min)	30	0.148	0.074	0.049	0.037
			45	0.222	0.111	0.074	0.055
			60	0.296	0.148	0.099	0.074

			75	0.369	0.185	0.123	0.092
			90	0.443	0.222	0.148	0.111
49	0.905156	Fan flow (L/min)		54.309	27.155	18.103	13.577
		Standard gas flow(L/min)	30	0.326	0.163	0.109	0.081
			45	0.489	0.244	0.163	0.122
			60	0.652	0.326	0.217	0.163
			75	0.815	0.407	0.272	0.204
			90	0.978	0.489	0.326	0.244

1.5 Gas analysis methods

1.5.1 Test and detection conditions

This experiment employed the nanoscale reagent spectrophotometric method to detect the NH_3 inlet concentration and outlet concentration, aiming to obtain the NH_3 removal efficiency. Additionally, a gas analyzer was used to analyze the generated nitrogen oxides, determining the residual content of NH_3 after treatment. Therefore, this experiment is a quantitative analysis experiment.

The EVOLUTION 201 UV spectrophotometer and a nitrogen oxide gas analyzer were utilized. Sampling was conducted at the inlet and outlet of the overall reaction system using U-shaped tube thin plate absorbers. [10] The nitrogen oxide gas analyzer was connected at the exhaust outlet.

1.5.2 Drawing of standard curves

To perform quantitative analysis of the collected ammonium sulfate solution in this experiment, a standard curve for ammonium ions calibrated with nanoscale reagent is needed. [11] The following procedure is used to simulate the standard curve using an ammonium chloride solution:

1) Prepare potassium sodium tartrate solution: Dissolve 50g of potassium sodium tartrate ($KNaC_4H_6O_6 \cdot 4H_2O$) in 100mL of water. Heat the solution to boiling to drive off ammonia, then let it cool and dilute to 100mL.

2) Prepare the ammonium standard stock solution (ammonium chloride solution): Weigh 0.7855g of ammonium chloride (NH4Cl, analytical grade, dried at 100-105°C for 2 hours) and dissolve it in water. Transfer the solution to a 250mL volumetric flask and dilute with water to the mark.

3) Take seven 10mL volumetric flasks with stoppers and prepare the standard series according to Table 4.

4) Accurately transfer the corresponding volumes of the standard solution into the volumetric flasks as specified in Table 4. Plot the calibration curve using the NH4+ content (μg) as the x-axis and the absorbance (at 420nm) after subtracting the blank absorbance as the y-axis. The resulting absorbance values for different standard concentrations of NH4+ are shown in Table 5.

Table 4: Matching chart

No.	0	1	2	3	4	5	6
Standard	0.00	0.10	0.30	0.50	1.00	1.50	2.00
Water	10.00	9.90	9.70	9.50	9.00	8.50	8.00
Vontent	0	2	6	10	20	30	40

Table 5: Calibration point table

concentration (mg/L)	0	0.2	0.6	1	2	3	4
absorbance	0	0.037	0.081	0.15	0.291	0.438	0.589

According to the above data, the absorbance is the ordinate, and the volume concentration (ppm) is used as the abscissa, and the standard curve is plotted, as shown in Figure 5. [12]

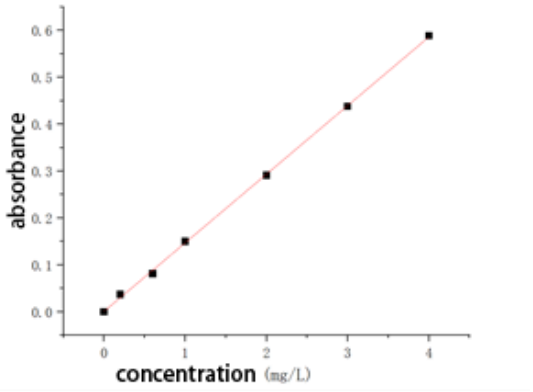

Figure 5: NH4+ standard curve

From the figure above, the$_{NH4}^{+}$ standard curve equation is as follows:

$$Y = 0.0146X + 0.0007 \quad (6)$$

where X is the logarithmic value of the volume concentration (ppm) and Y is the corresponding value of absorbance.

2. Result

In this chapter, we aim to explore the effects of different operating conditions on the removal of NH_3 by the reactor. By using the method of controlling variables, we analyze the four influencing factors: discharge voltage, discharge gap, inlet concentration, and residence time. We determine the importance of these different factors.

As this experiment involves high voltage, there is a certain level of risk involved. Therefore, it is necessary to conduct preliminary experiments to adjust and optimize the experimental procedures. To ensure safety, the maximum voltage applied to each reactor does not exceed its breakdown voltage. Therefore, the maximum voltages that can be applied for different discharge gaps are as follows: 23kV, 29kV, 33kV, and 38kV.

2.1 Effect of discharge voltage

Experimental conditions: The experiment was conducted at room temperature and atmospheric pressure. The corona wire was a single strand, with a residence time of 2 seconds and an inlet concentration of 60 ppm. Ventilation tests were conducted for four different discharge gaps, and the experimental results were plotted with removal efficiency (%) on the y-axis and discharge voltage (kV) on the x-axis, as shown in Figure 6.

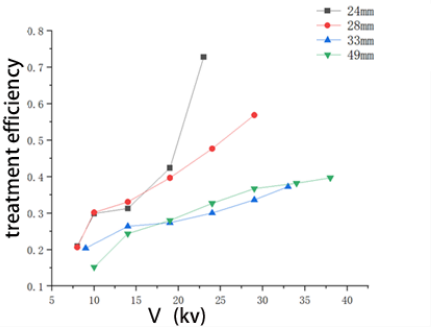

Figure 6: Influence of discharge voltage on removal efficiency

From the graph, it is evident that as the voltage increases, the removal efficiency of NH_3 increases continuously. In the absence of pressurization of the reactor, the average removal efficiency is around 15%, which is attributed to the adsorption effect of the stainless steel tube and PVC pipe. When the voltage reaches the corona onset

voltage, the reactor starts to produce corona, but the input energy is limited, resulting in weak gas discharge intensity and less significant removal effect, with an average removal efficiency of 15.6%. As the voltage approaches the breakdown voltage (23 kV, 29 kV, 33 kV, 38 kV), the removal efficiencies of NH_3 are 72.8%, 56.9%, 37.3%, and 38.2%, respectively.

Based on the above experimental results, the following conjectures can be made: With the increase of discharge voltage, the input energy into the reactor increases, and the gas discharge intensity becomes stronger, leading to an increase in the number of active particles (·OH, O_3, etc.) in the reactor. Consequently, the oxidation effect on NH_3 molecules becomes stronger. Simultaneously, after the voltage reaches a certain level, the number of active particles generated inside the reactor is sufficient to oxidize the majority of NH_3 molecules, resulting in no further significant increase in removal efficiency.

2.2 Effect of discharge gap

Experimental conditions: The experiment was conducted at room temperature and atmospheric pressure. The corona wire was a single strand, with a discharge voltage of 19 kV and an inlet concentration of 60 ppm. The flow rate was set according to the gas distribution table 3. The experimental results were plotted with treatment efficiency (%) on the y-axis and discharge gap (mm) on the x-axis, as shown in Figure 7.

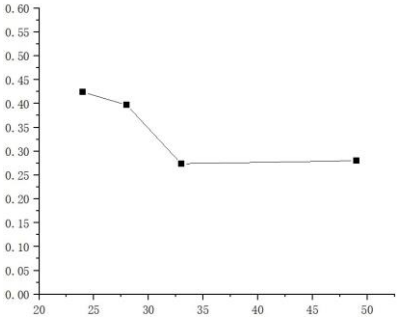

Figure 7: Influence of discharge gap on removal efficiency

The experimental results show that, at the same discharge voltage and inlet concentration, a larger discharge gap leads to poorer removal efficiency. However, when the discharge gap increased from 33 mm to 49 mm, there was no significant decrease in removal efficiency, and there was even a slight increase.

According to the analysis of the voltage-current characteristics in Chapter 3, it is known that at the same discharge voltage, a larger discharge gap leads to a smaller current. Many gas molecules are not sufficiently excited due to the increased discharge gap and therefore do not receive enough energy. As a result, the discharge region decreases significantly, leading to a decrease in the number of active components in the reactor. The fewer active particles generated in the reactor per unit of time, the lower the removal efficiency of NH_3. Additionally, as the discharge gap increases, the volume of the reactor also increases from 0.22 L to 0.91 L. This leads to a decrease in the density of active particles, reducing the probability of non-elastic collisions between NH_3 molecules and active particles, thereby reducing the removal efficiency of NH_3 gas.

2.3 Effect of dwell time

Experimental conditions: The experiment was conducted at room temperature and atmospheric pressure. The corona wire was a single strand, with a discharge voltage of 24 kV and an inlet concentration of 60 ppm. The discharge gap was kept constant, and different residence times of 1s, 2s, 3s, and 4s were tested. The experimental results were plotted with removal efficiency (%) on the y-axis and residence time (s) on the x-axis, as shown in Figure 8.

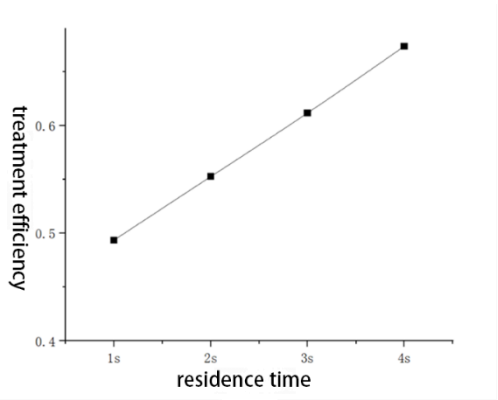

Figure 8: Influence of residence time on removal efficiency

As the residence time of NH_3 gas in the reactor increases, the removal efficiency continuously increases. The average removal efficiency increases from 49.4% to 67.4%, and a linear relationship is observed, meeting the removal requirement.

Under the same operating conditions, with the same discharge voltage and discharge gap, the energy output per unit time from the reactor is constant. Therefore, the rate of generating active particles is fixed. As the residence time increases, the total amount of active particles generated increases, resulting in an increase in the removal efficiency. In addition, increasing the residence time also increases the collision opportunity and reaction time between NH_3 molecules and active particles, leading to a higher removal efficiency of NH_3.

3. Discussion

1) In this experiment, only the theoretically analyzed best core (a single 0.1mm titanium wire) was selected for testing, and the removal efficiency of the four homemade reaction cores was not verified. Therefore, the accuracy of the computer software analysis could not be validated. In future studies, it would be beneficial to verify the removal efficiency of these four reaction cores to obtain practical results and support theoretical exploration.

2) In the analysis of influencing factors, this experiment did not consider the effect of inlet concentration on the reactor's efficiency, and orthogonal analysis was not used to investigate the impact of the four different factors on the reactor's treatment efficiency. In future analyses, it would be important to explore the influence of inlet concentration on the reactor's treatment performance and assess the relative importance of these four factors.

3) Detailed analysis of the reactor's power consumption and selection of the most suitable equipment for practical production were not conducted in this experiment. Future studies can focus on energy consumption analysis and optimal design to prepare for practical implementation.

4) Due to the presence of nitrogen in the air, quantitative analysis of reaction products was not possible in this experiment. In future studies, it would be helpful to use a mixture of inert gas and oxygen instead of air for easier quantitative analysis of the reaction products.

4. Conclusion

The main research findings are as follows:

1) Voltage: Voltage has a significant impact on the removal efficiency, where higher voltages result in better removal efficiency. Under specific conditions (24mm discharge gap, 23kV voltage, 3s residence time, and 60ppm inlet concentration), the NH_3 removal efficiency can reach 73%.

2) Discharge gap: In the same operating conditions, a larger discharge gap leads to lower removal efficiency for odorous gases. Under specific conditions (19kV voltage, 3s residence time), the highest average removal rate is achieved with a discharge gap of 24mm, reaching 42.4%.

3) Residence time: The residence time has a noticeable effect on the removal of odorous compounds, as increasing the residence time enhances the non-elastic collisions between odorous molecules and reactive particles, thus improving the removal efficiency. Under specific conditions (3s residence time, 24mm discharge gap, 19kV voltage), the average removal rate can reach 67.3%.

4) Energy consumption consideration: Without considering the reactor's energy consumption, the desired removal efficiency can be achieved by increasing the operating voltage and residence time. Moreover, increasing the residence time of reactants inside the reactor can also improve the removal efficiency.

In summary, by adjusting the discharge voltage, discharge gap, and residence time, it is possible to optimize the NH_3 removal efficiency in a high-voltage DC corona discharge reactor and provide guidance for practical applications. However, further experiments and analysis are needed to validate these conclusions, considering other influencing factors, in order to improve the application of this reactor in odor purification.

References

Li Mingshu. Catalyst synergistic discharge plasma for sulfur-containing odorous gas [D]. Hubei: Huazhong University of Science and Technology, 2009. DOI:10. 7666/d. d086734

Min X B, Zhou M, Chai L Y, et al. Treatment of nickel-ammonia complex ion-containing ammonia nitrogen wastewater [J]. Transactions of Nonferrous Metals Society of China, 2009(05):334-338. [3] Hansgen D A, Vlachos D G, Chen J G. Using first principles to predict bimetallic catalysts for the ammonia decomposition reaction[J]. Nature Chemistry, 2010, 2(6):484-489.

Blázquez E, Bezerra T, Lafuente J, et al. Performance, limitations and microbial diversity of a biotrickling filter for the treatment of high loads of ammonia [J]. Chemical Engineering Journal, 2017, 311: 91-99.

Zhang Tiantian, Li Jianjun, Cen Yinghua, et al. Study on biomembrane purification of biological drip filter with low concentration and high air volume odorous gas [J]. Microbiology China, 2007, 34(6): 1052-1056. Seguel. Environmental Pollution. 2013.

Langmuir I, Tonks A. General theory of the plasma of an arc [J]. Physical Review, 1929, 34(06): 876-922.

Zhang F G. Control of ammonia and odors in animal houses by a ferroelectric plasma reactor [J]. IEEE Transaction on Industry Application, 1993, 17(06): 20-31

Dai Huixiang, Lu Wenjing, Yawar Abbas, et al. Removal of ammonia from simulated compost gas by two-dielectric barrier discharge low-temperature plasma [J]. Chemical Industry and Engineering Progress, 2020, 39(9):3801-3809.) DOI: 10. 16085/j. issn. 1000-6613. 2019-1851.

Ulien J, Pierre V. Decomposition of gaseous sulfide compounds in air by pulsed corona discharge [J]. Plasma Chemistry and Plasma Processing, 2007, 27(03): 241-255.

Nie Yong, Li Wei, Shi Yao et al. Study on treatment of malodorous gas in refinery by pulse discharge plasma [J]. Journal of Environmental Science, 2004, (04): 672-677.

Fu Lili, Liu Tianhui, Jiang Binhui, et al. Experimental study on ammonia removal by atomization synergistic low-temperature plasma[J]. Environmental Engineering, 2016, 34(7):125-128. DOI: 10. 13205/ j. hjgc. 201607026.

Lu, S., Chen, L., Huang, Q., Yang, L., Du, C., Li, X., & Yan, J. (2014). Decomposition of ammonia and hydrogen sulfide in simulated sludge drying waste gas by a novel non-thermal plasma. Chemosphere, 117, 781-5.